Tectonophysics xxx (2010) xxx–xxx

Contents lists available at ScienceDirect

Tectonophysics

journal homepage: www.elsevier.com/locate/tecto

Towards incorporating uncertainty of structural data in 3D geological inversion

J. Florian Wellmann [a,*], Franklin G. Horowitz [a], Eva Schill [b], Klaus Regenauer-Lieb [a,c,*]

[a] Western Australian Geothermal Centre of Excellence, School of Earth and Environment, The University of Western Australia, 35 Stirling Hwy, WA-6009 Crawley, Australia
[b] Université de Neuchâtel, Institut de géologie et hydrogéologie, Rue Emile-Argand 11, CH-2009, Neuchâtel, Switzerland
[c] CSIRO ESRE, PO Box 1130, Bentley, WA-6102, Australia

ARTICLE INFO

Article history:
Received 28 September 2009
Received in revised form 16 March 2010
Accepted 19 April 2010
Available online xxxx

Keywords:
Uncertainty
Implicit 3D geological modelling
Geological inversion
Potential-field interpolation
Raw data quality
Visualisation

ABSTRACT

All geological models are subject to several kinds of uncertainty. These can be classified into three different types: data imprecision and quality, inherent randomness and incomplete knowledge. With our approach, we address uncertainties introduced by input data quality in complex three-dimensional (3D) models of subsurface structures (geological models). As input data, we consider parameters of geological structures, i.e. formation and fault boundary points and orientation measurements.

Our method consists of five steps: construction of an initial geological model with an implicit potential-field method, assignment of probability distributions to data positions and orientation measurements, simulation of several input data sets, construction of several model realisations based on these simulated data sets and finally the visualisation and analysis of the uncertainties.

We test our approach in two generic models, a simple graben setting and a complex dome structure. The first model shows that our approach can evaluate uncertainties from different structures and their interaction. Furthermore, it indicates that the final uncertainty of the model is not simply the sum of all input data uncertainties but complex interactions exist. The second example demonstrates that our approach can handle full three-dimensional settings with overturned surfaces.

Results of the uncertainty simulation can be visualised and analysed in several ways, ranging from borehole histograms to uncertainty maps. For complex 3D visualisation and analysis, we use indicator functions. When we apply these, we can treat the visualisation of uncertainties in complex settings in a self-consistent manner.

With our simulation method, it is possible to analyse and visualise the uncertainties directly introduced by imprecision in the input data. Our approach is intuitive and straight-forward and suitable in both simple and complex geological settings. It enables detailed insights into the model quality, even for the non-expert. In cases where a geological model is the basis for geophysical simulation, it opens-up the way to geological data-driven ensemble modelling and inversion.

1. Introduction

Three-dimensional models of the subsurface structure (geological models) require quality estimation for interpretation and further use. To date, no comprehensive 3D approach exists to assess uncertainties in a geological model (Turner, 2006). Here, we present a statistical simulation method aiming to assess and communicate the accuracy of complex 3D geological models based on uncertainties in the input data. As input data, we denote here data typically used for structural modelling, i.e. contact points for formation and fault surfaces and orientation measurements.

Our uncertainty evaluation differentiates itself from previous approaches (e.g. Thore et al., 2002; Tacher et al., 2006; Bistacchi et al., 2008; Suzuki et al., 2008) since we do not consider a probabilistic measure of the quality of the raw data in the final model. Rather, we directly simulate the effect of data uncertainty in full 3D. This complements and extends typical geostatistic procedures (e.g. Chilès and Delfiner, 1999; Deutsch, 2002) and is a first step towards 3D geological inversion.

Our technique is based on a recent geological modelling method (Calcagno et al., 2008; Guillen et al., 2008). Their method allows model construction directly from input data, once all parameters are defined. It also incorporates geological laws and is capable of dealing with complicated geological settings like domes and overturned folds (Fig. 1).

1.1. Structural modelling methods

3D structural modelling usually aims to create a digital model representing the geometry of structures in the subsurface, from a microscale to a crustal scale. The modelling is typically based on different types of data like boreholes, geological maps or seismic reflection surveys.

* Corresponding authors. J.F. Wellman is to be contacted at Western Australian Geothermal Centre of Excellence, The University of Western Australia, 35 Stirling Hwy, WA-6009 Crawley, Australia. Tel.: +61 8 6488 7230; fax: +61 8 6488 1050. K. Regenauer-Lieb, CSIRO ESRE, PO Box 1130, Bentley, WA-6102, Australia.
E-mail addresses: wellmann@cyllene.uwa.edu.au (J.F. Wellmann), Klaus.Regenauer-Lieb@CSIRO.au (K. Regenauer-Lieb).
URL: http://www.geothermal.org.au (J.F. Wellmann).

0040-1951/$ – see front matter © 2010 Elsevier B.V. All rights reserved.
doi:10.1016/j.tecto.2010.04.022

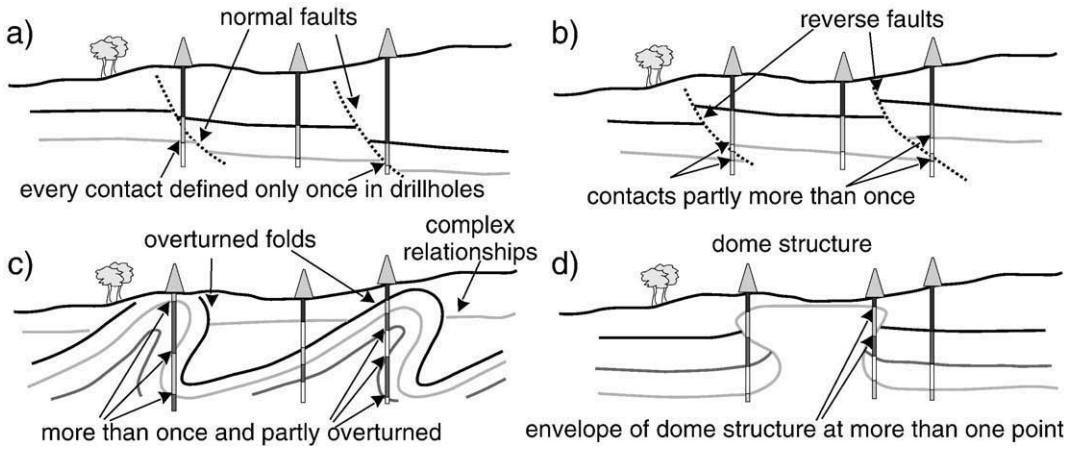

Fig. 1. Simple and complex geological settings in a modelling sense; (a) normal faulting in a layer-cake model, e.g. a basin setting; no complications for elevation surface modelling methods, (b) reverse faulting, e.g. an inverted basin; due to the reverse faulting, formations are doubled at some locations, (c) overturned fold; again, the folded formation exists at more than one (x,y) point in space; the same applies for (d) a salt dome or magmatic intrusion.

There are several approaches to the construction, modelling and representation of geological objects. These approaches mostly differ in the details of their interpolation of data and in their ability to represent complex structures in 3D. Several common approaches represent geological structures as elevation surfaces (see Fig. 1a). Here, one point on a surface is associated to a specific reference (u,v), for example a geographic position. The coordinates of the point are calculated with functions (usually polynomial) for each coordinate direction, e.g. $x=f_1(u,v), y=f_2(u,v), z=f_3(u,v)$. In these cases, the surface can be imagined as a plane that can be completely projected onto the flat reference plane. These interpolation methods are sometimes referred to as 2.5D methods (e.g. MacEachren et al., 2005; Wu et al., 2005; Bistacchi et al., 2008; Caumon et al., 2009). However, the term 2.5D can be ambiguous as it is also used to describe methods where the geology is defined in a section (e.g. a X–Z-section) and with extrusion perpendicular to it (in Y-direction) as done for section balancing (e.g. Galera et al., 2003; Moretti, 2008) or geophysical modelling (e.g. Sander and Cawthorn, 1996; Malengreau et al., 1999; Truffert et al., 2001).

Geostatistical approaches can be applied (e.g. Goovaerts, 1997; Chilès and Delfiner, 1999), allowing for more geologically reasonable results. A drawback of these techniques is their difficulty in handling some complex geological structures such as reverse faulting (Fig. 1b), overturned folding (Fig. 1c), or the complexities of doming structures (Fig. 1d). For such structures, approaches that can handle structures independent of their orientation are required. One common approach is the construction of triangulated irregular nets (TINs). The geological structure is interpolated explicitly between defined points and it is possible to model any type of structure. These surface methods are implemented in a variety of software packages (e.g. Turner, 2006; Howard et al., 2009; Kessler et al., 2009; Wycisk et al., 2009). Similar approaches have been developed for direct volume construction using Voronoï cells (Courrioux et al., 2001). However, for complex structures, closely spaced sections and a high data density are required.

Implicit function techniques overcome some of these limitations. In such techniques, geological surfaces are represented as isovalues of certain functions defined everywhere in space. The functions are constructed from the locations and attitudes of measured data points, along with other external constraints (e.g. Mallet, 1992; Lajaunie et al., 1997; Frank et al., 2007). These methods are commonly used in various geological modelling packages. Specifically, for our uncertainty simulations, we apply the implicit function approach that is based on an interpolation of a harmonic potential field (Lajaunie et al., 1997; Calcagno et al., 2008). This approach enables the fast construction of a model directly using position and orientation data. This is described in more detail below (Section 2.2).

1.2. Uncertainties in structural modelling

Almost all types of geological data are subject to several sources of uncertainty (e.g. Mann, 1993; Davis, 2002). These include measurement inaccuracies, sampling limitations, insufficient sample numbers, imperfect concepts and hypotheses, the need for simplifications, heterogeneity, inherent randomness and many others. These different types of uncertainties can be broadly separated into three categories (Cox, 1982; Mann, 1993; Bárdossy and Fodor, 2001): (1) imprecision and measurement error, (2) stochasticity, and (3) imprecise knowledge.

We adapt the classification of Mann (1993) to the case of structural modelling. Typical examples are presented in Fig. 2:

Type 1 (error, bias, and imprecision): uncertainty in all types of raw data that are used for modelling, like the position of a formation boundary or the orientation of a structure (Fig. 2a).

Type 2 (stochasticity, and inherent randomness): this commonly shows up as the uncertainty in interpolation between (and extrapolation from) known data points (Fig. 2b).

Type 3 (imprecise knowledge): applies to incomplete and imprecise knowledge of structural existence, general conceptual ambiguities and the need for generalisations (Fig. 2c).

In the current literature, a comprehensive treatment of all types of uncertainties in 3D structural geological modelling is still lacking. Type 1 uncertainties can be handled with geostatistical methods for simple structures (Chilès and Delfiner, 1999). Even when the gross uncertainties have been reduced with seismic data, the remaining uncertainty affects the resulting models (e.g. Thore et al., 2002; Glinsky et al., 2005). But to date, there is no method to evaluate the influence of different data uncertainties, including orientation measurements, in complex geological settings.

Uncertainties of Type 2 have been addressed with a variety of statistical and geostatistical methods (Chilès and Delfiner, 1999; Deutsch, 2002; Davis, 2002, and others). Uncertainties of Type 3 are more difficult and sometimes impossible to evaluate (e.g. Mann, 1993; Bárdossy and Fodor, 2001).

Generally, all three types of uncertainties can be addressed by the formulation of a suitable inverse problem. With the method presented here, we are concentrating on Type 1 uncertainties, based on error, bias

Please cite this article as: Wellmann, J.F., et al., Towards incorporating uncertainty of structural data in 3D geological inversion, Tectonophysics (2010), doi:10.1016/j.tecto.2010.04.022

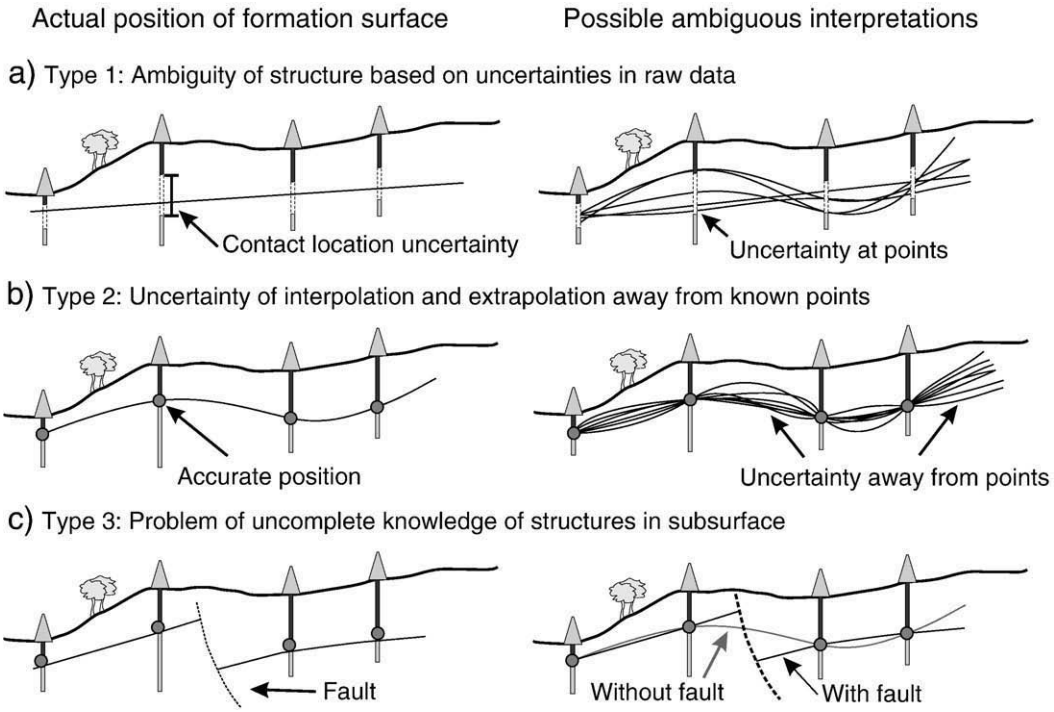

Fig. 2. Adapting the classifications of Mann (1993) to the uncertainties in structural modelling; (a) interpretation of a geological formation boundary based on ill-defined input data points (i.e. where the contact position itself is uncertain) and resulting uncertainty in the interpreted boundary, (b) uncertainty of interpolation between and extrapolation away from known data points, (c) incomplete knowledge of structures in the subsurface, e.g. does a fault exist or not.

and imprecision. But the method is equally suitable to analyse special cases of Type 3 uncertainties (see Discussion and Appendices A).

2. Materials and methods

2.1. Method overview

We define geological uncertainties in the following section as uncertainties based on the position, orientation, and interpretation of contextual geological information and data. We also explicitly investigate the influence of raw data uncertainties on the model quality while assuming that the applied interpolation is correct (see Discussion).

Our procedure to simulate uncertainty in a model is simple and straightforward. It can generally be separated into five steps (see Fig. 3):

Step 1. Construction of an initial 3D geological model. This model is considered as the best possible model that can be constructed using all available input data (formation and fault positions and orientation measurements). All relevant modelling parameters are defined in this model (e.g. model extent, geographic projection, and digital elevation model) as well as the fault network and the stratigraphy.

Step 2. Identification of the input data quality and assignment of probability distributions. This can be based on either direct observations or statistical inference and educated guess (see below). Both data positioning and orientation uncertainties can be considered.

Step 3. Simulation of several input data sets based on the raw data in the initial model and the assigned probability distributions of the previous steps.

Step 4. Construction of multiple geological model representations with the simulated input data sets.

Step 5. Visualisation, processing and analysis of results.

All important steps are described in detail below.

2.2. Construction of the initial geological model

The initial model is the starting point for our analysis. We apply an implicit potential-field approach for the geological modelling (Lajaunie et al., 1997). The interpolation itself is based on universal cokriging (Chilès et al., 2004). It is implemented in the software GeoModeller/Éditeur Géologique developed by BRGM and Intrepid Geophysics (http://www.geomodeller.com). In two recent publications, Calcagno et al. (2008) and Guillen et al. (2008) describe all relevant features. The method has been applied in complex geological settings (e.g. Martelet et al., 2004; Maxelon and Mancktelow, 2005; Joly et al., 2008) and produces reasonable geological models based on limited input data (Putz et al., 2006).

The main advantage of this approach is that geological models are created based directly on the geological contact and orientation data — once the model is setup and structural and stratigraphic relationships are defined (Calcagno et al., 2008). It is thus possible to regard a geological model $\mathscr{M}$ solely as a computed function $\mathcal{C}$ of the input data set $\boldsymbol{k}$ as

$$\mathscr{M} = \mathcal{C}(k_1, k_2, \ldots, k_n) = \mathcal{C}(\boldsymbol{k}). \quad (1)$$

The components k_i of the input data set can be any one coordinate x, y or z of a boundary point $P(x,y,z)$ or the location or attitude parameters (azimuth φ and dip θ) of a structural measurement $O(x, y, z, \varphi, \theta)$ for both formations and faults.

The ability to directly model the effect of a changed or augmented input data set – even in complex geological settings while honouring defined stratigraphic relationships and fault systems – makes this approach an ideal tool for our uncertainty simulation.

2.3. Probability distributions for input data

The next step is identifying uncertainties and assigning probabilities to the model input data set **k**. Geological and geophysical data used for modelling are never absolutely accurate (e.g. Davis,

Please cite this article as: Wellmann, J.F., et al., Towards incorporating uncertainty of structural data in 3D geological inversion, Tectonophysics (2010), doi:10.1016/j.tecto.2010.04.022

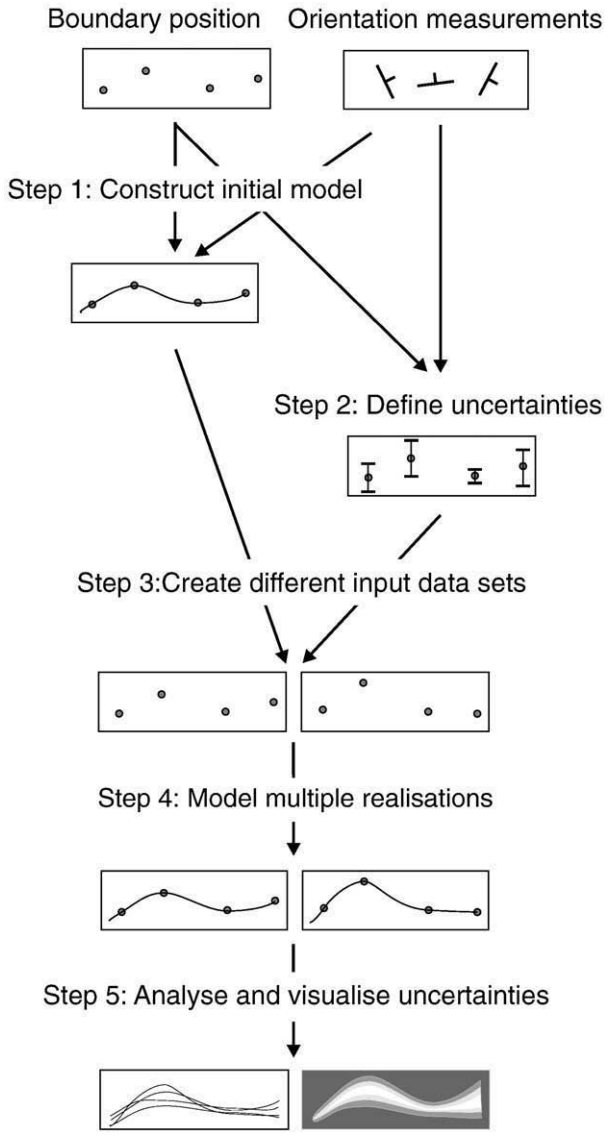

Fig. 3. Simplified work-flow for the five steps of our approach: (1) Initial model construction from formation boundary position and orientation measurements and (2) defined probability distributions are used to (3) simulate different data sets for (4) multiple model realisations. These are then processed to (5) analyse and visualise model uncertainties.

2002). Uncertainties range from the position at the surface to the estimation of dip angles at depth. All types of uncertainty have a specific effect on a 3D model depending on model scale and complexity. An uncertainty of 10 m may be irrelevant in a model at regional scale but significant for a high-resolution local-scale model.

Every geologist is well aware of the raw data problems encountered when constructing maps and cross-sections. Geophysicists know of similar problems, for example when processing seismic data. It may be possible to derive a probability distribution directly from repeated measurements, for example for variation of dip and strike in orientation measurements. For example, Bistacchi et al. (2008) present some considerations about uncertainty quantification related to faults and folds when observed in the field. Other aspects of uncertainties in raw data have also been analysed, e.g. for seismic processing (Thore et al., 2002; Glinsky et al., 2005) and for the problem of geological complexity (Tacher et al., 2006). Still, a general quantitative treatment of uncertainties in the context of structural modelling is not available to date. Therefore, probability distributions sometimes have to be assigned based on heuristic knowledge and educated guess.

In our uncertainty simulation, we consider the positions of bounding points and orientations of bedding or other planar elements in formations and faults. These points and orientations can be derived from any type of data (outcrop observations, seismic data, and boreholes).

In many geological situations, it is reasonable to express the uncertainty as a normal distribution with a standard deviation σ around an expected value μ (e.g. Davis, 2002). A typical case is that the contact between two formations in a drillhole or outcrop is not easily recognised (see Fig. 4a).

In our approach, we usually assume the expected value of the probability distribution to be the data value of k_i of the initial model. The probability distribution for a value ξ_i drawn from this population is then

$$p(\xi_i) = \frac{1}{\sigma\sqrt{2\pi}} e^{-\frac{(\xi_i - k_i)^2}{2\sigma^2}}. \quad (2)$$

But even if a normal distribution is commonly used, other statistical distributions may also be reasonable in geological circumstances. A continuous uniform distribution should be used where all points in a finite interval are equally probable. This might be the case when a contact between two formations is not outcroping or when a segment is missing in a drillhole (see Fig. 4b), expressing the notion that there is no reason to assume that a boundary located at one point is more likely than at another. The probability distribution for one point k_i with an uncertainty range of a in both directions can then be described as

$$p(\xi_i) = \begin{cases} \frac{1}{2a} & \text{for } k_i - a \le \xi_i \le k_i + a \\ 0 & \text{for all other cases.} \end{cases} \quad (3)$$

Another typical case is that some discrete points are possible positions for one data point. In this case, a probability α_i can be assigned to every possible discrete value such that

$$\sum_i \alpha_i = 1. \quad (4)$$

An example is the determination of a geological contact out of a wireline well-log (e.g. gamma-ray log). Often, an uncertainty exists of which peak in the log might correspond to the exact contact even if every peak itself is well defined (see Fig. 4c). If, for example, there are two possible positions for one parameter, with a probability of $\alpha_1 \in [0,1]$ for the first position (which can be the position in the base model, k_i) and a probability of $\alpha_2 = 1 - \alpha_1$ for the second position (with an offset of b to k_i), we can describe the discrete probability distribution as

$$p(\xi_i) = \begin{cases} \alpha_1 & \text{for } \xi_i = k_i \\ \alpha_2 & \text{for } \xi_i = k_i + b \\ 0 & \text{for all other cases.} \end{cases} \quad (5)$$

In other cases, a combination of the above described probability distributions might be required, for example a normal distribution for two different mean values at two possible, but inexact, positions along the well-log. Another distribution which is applicable for some types of geological data is the lognormal distribution (e.g. Davis, 2002).

Special care has to be taken for the implementation of dip and azimuth uncertainties. For simple cases with small angular changes not too close to 0° and 90°, a statistical distribution like the ones discussed above can be used. In more complex cases, a spherical distribution should be applied (Fisher, 1953; Davis, 2002).

Please cite this article as: Wellmann, J.F., et al., Towards incorporating uncertainty of structural data in 3D geological inversion, Tectonophysics (2010), doi:10.1016/j.tecto.2010.04.022

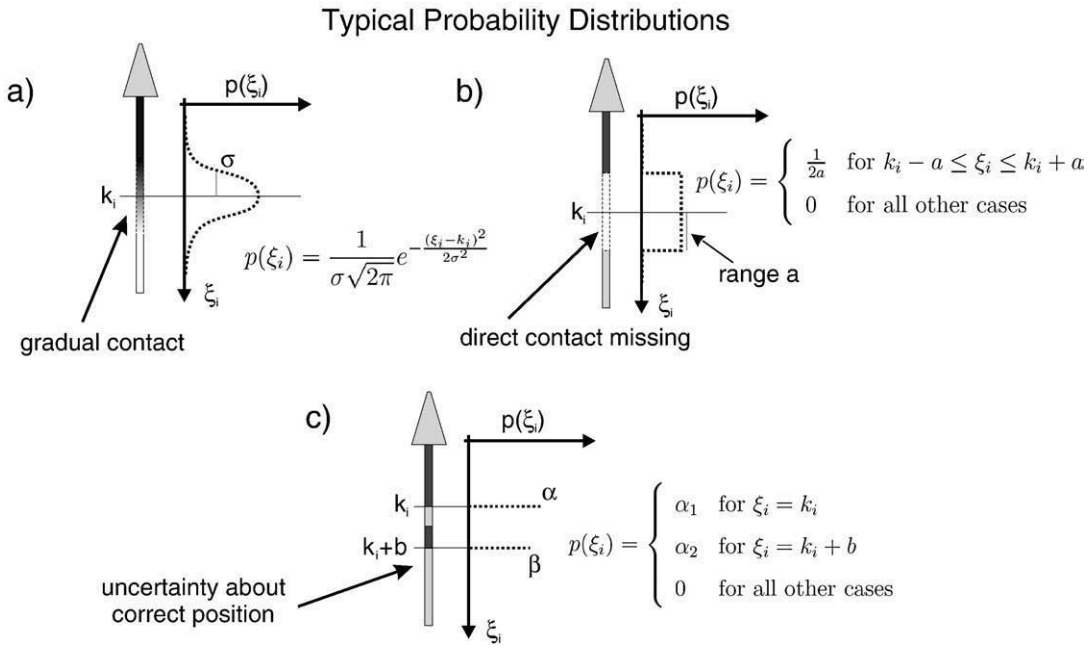

Fig. 4. Examples of problems for the direct determination of a formation boundary and possible probability distributions, e.g. in a drillhole: (a) contact is gradual: normal distribution, (b) contact itself is missing or its position is uncertain: continuous uniform distribution, (c) two (or more) discrete positions for a contact are possible: discrete probability distribution.

2.4. Simulation of different input data sets

After the initial model is set up and uncertainties of orientation and contact data are evaluated, we can start the simulation of new input data sets. This is performed in a straight-forward way:

Step 1. We use our initially created base model $\mathscr{M}_{\text{base}}$ and its data set $\boldsymbol{k}_{\text{base}}$ as starting point for our simulation (see Section 2.2). This base input data set consists of surface and boundary positions of formations or faults, and the position and attitude of structural measurements. All or a subset of these values can be changed. All modelling parameters (e.g. model space, formations, etc.) are kept during the simulation.

Step 2. For every simulation run ν of a total number of simulations n, we create a new model data set $\boldsymbol{k}_\nu$ where every data point $k_{i,\nu}$ of the set $\boldsymbol{k}_\nu$ represents a random sampling from its associated probability distribution

$$k_{i,\nu} = p(\xi_i) \tag{6}$$

Step 3. We repeat step 2 to create n new data sets. The number of created data sets depends on the required level of significance for the analysis and the available computation power (see below).

Step 4. We compute a geological model $\mathscr{M}_\nu$ for every simulated data set:

$$\mathscr{M}_\nu = \mathcal{C}(\boldsymbol{k}_\nu) \tag{7}$$

Step 5. After creating these different models, we can compare model results or process the models for visualisation.

The simulation workflow is implemented in a python module to process the original input data structure and create new input data sets that can directly be recomputed. The workflow itself is also suitable for computational parallelisation. The complete uncertainty simulation process would then only take slightly longer than a normal model run.

The n realisations of the model all represent possible subsurface models given the initial model and assigned data probability distributions. We can now use statistical methods to analyse and display the model uncertainties.

2.5. Analysis and visualisation

The choice of methods to analyse and visualise the simulated uncertainties depends on the complexity of the geological setting, the model configuration, and the further use of the model. We can distinguish between an overall visualisation of the model uncertainties, the analysis of uncertainty of a specific model feature and the processing of all model realisations to further simulation and inversion tools.

Different approaches to visualise location uncertainties have been proposed and discussed in literature (see MacEachren et al., 2005, for an extensive review). These approaches are mainly developed for map representations. Similarly, Viard et al. (2007) have developed techniques to represent uncertainties in stratigraphic grids, specifically suited for geological and petrophysical parameters. Still, even if displayed in 3D, these analyses are only suitable for elevation surface/2.5D situations.

Most of these visualisation concepts can be extended for 3D analyses, for example maximum likelihood, multiple realisations and multinominal probability fields (Goodchild et al., 1994). We present here the application of standard approaches and propose specific adaptations to 3D setting.

A useful method is to display the results of all model realisations simultaneously (e.g. Goodchild et al., 1994; MacEachren et al., 2005). For example, it can be convenient to plot all simulated formation top surfaces in one cross-section or map. This delivers a good first insight into the effect of uncertainty on the model. A similar possibility is to plot all model realisations along a virtual drillhole at a location.

Simple analyses of the uncertainties can be based on these visualisations. For example, we can evaluate the min/max surfaces of formations and plot them into cross-sections, map-views and along virtual drillholes. We can extend this into three dimensions and calculate the min/max envelope surfaces of all realisations.

Please cite this article as: Wellmann, J.F., et al., Towards incorporating uncertainty of structural data in 3D geological inversion, Tectonophysics (2010), doi:10.1016/j.tecto.2010.04.022

Further analyses and visualisations are possible using statistical evaluations. One suitable analysis is the determination of the median for a modelled structure, e.g. a formation top, out of all realisations. Assuming a normal distribution of a simulated surface, it is furthermore possible to calculate a mean surface and the standard deviation at every point in space.

In simple cases where the structure can be treated as an elevation surface (Fig. 1a), it is convenient to visualise these analyses in a map view (e.g. MacEachren et al., 2005). But if the structural setting of the model is more complex, this is no longer possible and we need special procedures to analyse and visualise uncertainties. One suitable method is the use of indicator functions as the basis for further analyses. The indicator function of a formation F is a subset of the whole model space defined as

$$I_F(\boldsymbol{x}) = \begin{cases} 1 & \text{for } x \in F \\ 0 & \text{for } x \notin F \end{cases} \tag{8}$$

for all points $\boldsymbol{x}$ in the model domain. For practical reasons, we can quantize every model realisation onto a grid and calculate the indicator function for every grid cell $\mathcal{G}$. For the n simulated models, we thus obtain n indicator fields $I_{F_v}(\mathcal{G})$ for every modelled formation. This formal definition allows for a wide range of further analyses. For example, the minimal and maximal extent of a structure in its discretised grid form can be expressed as indicator fields $I_{F\min}$ and $I_{F\max}$ and directly be calculated as

$$I_{F_{\min}}(\mathcal{G}) = \prod_{k \in n} I_{F_k}(\mathcal{G}) \tag{9}$$

and

$$I_{F_{\max}}(\mathcal{G}) = 1 - \prod_{k \in n} \left(1 - I_{F_k}(\mathcal{G})\right). \tag{10}$$

Where $(1 - I_{F_k}(\mathcal{G}))$ is the complement of the indicator function.

We can also use the indicator functions to derive an indicator probability function $P_F(\mathcal{G})$ [0,1] for every formation in space. This function contains probability estimates for the formation represented by the indicator at every location and can be derived from the mean value of the local indicator functions as

$$P_F(\mathcal{G}) = \sum_{k \in n} \frac{I_{F_k}}{n}. \tag{11}$$

This definition is similar to the multinominal probability field definition of Goodchild et al. (1994). The result is a scalar field in three dimensions and we can use it to derive a contour of a probability threshold for one formation, e.g. the 95% probability to encounter a formation. This can be visualised as an isosurface in 3D or as 2D isolines in a section.

We can use the probability indicator field for a more detailed analysis of accuracy. The gradient of this field, ∇P_F, is a vector field pointing out the main direction and rate of change at every point in space. If we take the absolute value of this vector field

$$A_F = \|\nabla P_F\| \tag{12}$$

we obtain an estimate in full 3D space about the total rate of change in the probability field. Coming back to our goal, i.e. the identification of accuracy in the model, we can interpret the derived scalar field A_F as:

- High values ⇒ steep gradient in the indicator probability field ⇒ high probability to encounter the boundary of formation F
- Low values ⇒ shallow gradient in the indicator probability field ⇒ low probability to encounter the boundary of formation F.

If we apply this method to all formations, it gives us a direct indication of the overall accuracy in the whole model domain.

Another possible evaluation of uncertainties in more complex cases is to analyse a specific feature of the model, for example the volume of a modelled formation. One way to calculate the total volume of a formation is again based on the indicator functions defined above (Eq. (8)). We can estimate the total volume of a formation as the sum over all grid cells multiplied by the grid cell volume:

$$V_{F_v} \approx \sum_{g \in \mathcal{G}} \left\{ I_{F_v}(g) V(g) \right\}. \tag{13}$$

Taking the volume of all simulated models for one formation, we can perform further statistical evaluations, plot volume histograms for all realisations or use these results directly in business models that rely on an estimate of this property, for example ore tonnage.

3. Results

We apply our method to two generic 3D geological models. The first model is a typical example of a graben structure with tabular sedimentary formations cut by normal faults. This is a simple setting (in a modelling sense) and all analyses and visualisations can be performed on an elevation surface basis (see Fig. 1a). The second example is a dome structure, and is more challenging in both modelling and visualisation as complex relationships between structures exist (see Fig. 1d).

Both examples are common geological structures. Even if simplified for the purposes of this work, they are ideal to demonstrate the relevant steps in our uncertainty evaluation, possible applications, and challenges of analysing and visualising the results.

For a detailed description of all aspects concerning the modelling itself, please refer to Calcagno et al. (2008).

3.1. Simple graben model

3.1.1. Model setup

With our first example, we want to demonstrate the application of our uncertainty evaluation in a simple 3D geological model. The geological setting is a graben structure with non-planar normal faults cutting and displacing sub-horizontal sedimentary formations (Fig. 5). In terms of modelling, this is an elevation surface setting that could be treated with many typical modelling methods (see Section 1.1). All data are defined in two cross-sections (insets in Fig. 5) which could, for example, be derived from seismic cross-sections. The contact points are at the top surface of a formation or fault, structural symbols indicate orientation of faults and geological surfaces at these positions. General modelling settings are that the formation surfaces of the sedimentary pile are sub-parallel. The model stratigraphy consists of four onlapping formations, Formation 1 (oldest) to Formation 4 (cover layer, transparent in Fig. 5). Both faults are infinite in extent and affect all formations. The model covers an area of 2000 m in East–West direction, 1500 m in North–South and has a depth of 1000 m from the surface.

3.1.2. Simulation parameters and settings

After the initial model is constructed, we can introduce uncertainties for the input data (contact points and orientations) in the cross-sections. In this simple case, we want to consider two types of uncertainties:

1. The depth of the formation surface: assuming that we obtained the basic information for our cross-section from a 2D seismic line, it is reasonable to infer an error in the exact depth of a formation (e.g. due to an inaccurate time–depth conversion). This error is

Please cite this article as: Wellmann, J.F., et al., Towards incorporating uncertainty of structural data in 3D geological inversion, Tectonophysics (2010), doi:10.1016/j.tecto.2010.04.022

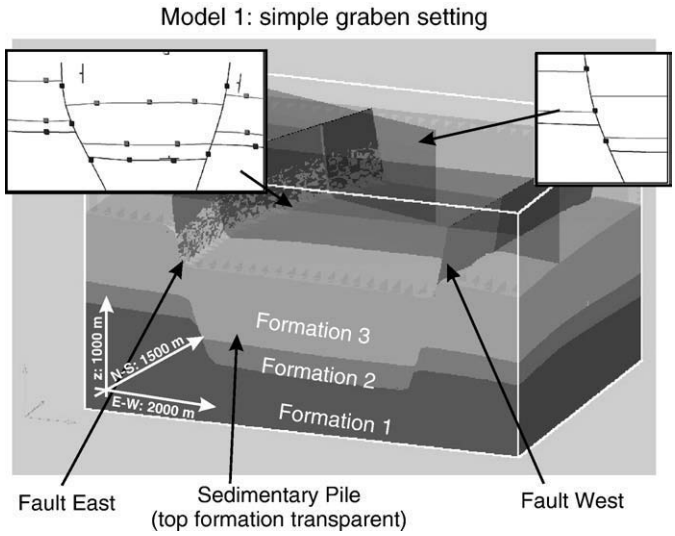

Fig. 5. Evaluation Model 1: simple graben setting, sedimentary sequence cut by two faults; data are defined in the cross-sections (insets).

similar for all data points of one formation and we assume that it increases with depth.

2. The lateral extension of the formations: we can assume that the dip of the fault surfaces defined in the 2D section is subject to an error perpendicular to the section as we do not have any other information about it.

We could also include further uncertainties, specifically the position of the faults at the surface and the position of the orientation measurements. But we intentionally kept this example simple to highlight the interaction of the above described uncertainties.

In a real geological model, the imprecision that would be assigned to the data can be identified directly from the source (see Section 2.3) or estimated with an educated guess, ideally supported by additional information (like the general geological setting, etc.). In this model, we assign a normal distribution (Eq. (2)) to the data points. As an estimate for the mean value of the distribution, we take the data value of the initial model. The assigned standard deviations for the distribution are noted in Table 1. For these example models, we perform 20 simulation runs.

3.1.3. Analysis and visualisation of results

A first good insight into the effect of uncertainties on the model can be obtained if we plot all surface intersections on one cross-section (Fig. 6a). As expected, the surfaces of all simulated models vary most for the bottom formation (Formation 1) which had the largest standard deviation. Another representation that provides a quick and easily interpreted visualisation is a histogram view of surface occurrences in a virtual well (Fig. 6b). We determine the depth value of all simulated surfaces at one location and plot these in histogram view. This can, for example, be used to communicate model uncertainties at a proposed drilling location.

Table 1
Estimations of the standard deviation assigned to the data in the graben model.

Formation	Data type	Direction	Stdev
Formation 1	Surface contact point	Depth (z)	30 m
Formation 2	Surface contact point	Depth (z)	20 m
Formation 3	Surface contact point	Depth (z)	10 m
Formation 1	Orientation	Dip angle	5°
Fault E	Orientation	Dip direction	5°
Fault W	Orientation	Dip direction	10°

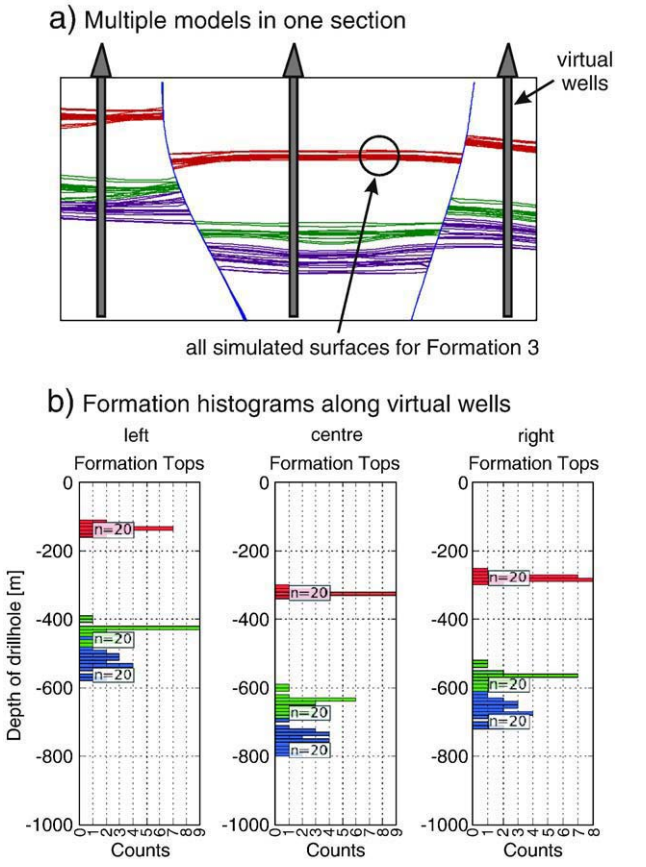

Fig. 6. Visualisation of results for Evaluation Model 1, simple visualisation: (a) visualisation of multiple models within one cross-section; (b) Histogram of formation depth along virtual wells.

We can extend the analysis of our results into a map view. This is possible in this case since we have a geological setting which can be represented with elevation surfaces and at every geographical point, there is only one surface point at depth (see Fig. 1a). If we analyse all simulated surfaces of one formation statistically, assuming a normal distribution of results, we can determine the standard deviation of the simulated surfaces in a map view. Fig. 7a shows an example of this method for Formation 3, projected onto the mean of all simulated surfaces. We can see that the areas of highest uncertainties correspond to the intersections of the formation surface with faults in the model as, of course, we would expect in this simple case. Still, it is important to note that the standard deviations exceed the input standard deviations (10 m for Formation 3). This can also be visualised in a histogram of local standard deviations (Fig. 7b) and is mainly due to the high fluctuations around the faults. The analysis shows how different uncertainties interact in the model: the uncertainty in the resulting model is not simply equal to the standard deviation (or any other probability distribution) in the input data.

3.2. Doming structures

3.2.1. Model setup

With the second model, we apply our approach to a more complex situation, both in the geological setting and in the interpretation of the results. We model a doming structure (for example a salt dome or a magmatic structure, called dome unit in the following) that is cutting through a sequence of sub-horizontal formations (for example a sedimentary sequence). This setting is more complex than the previous one as the boundary of the doming

Please cite this article as: Wellmann, J.F., et al., Towards incorporating uncertainty of structural data in 3D geological inversion, Tectonophysics (2010), doi:10.1016/j.tecto.2010.04.022

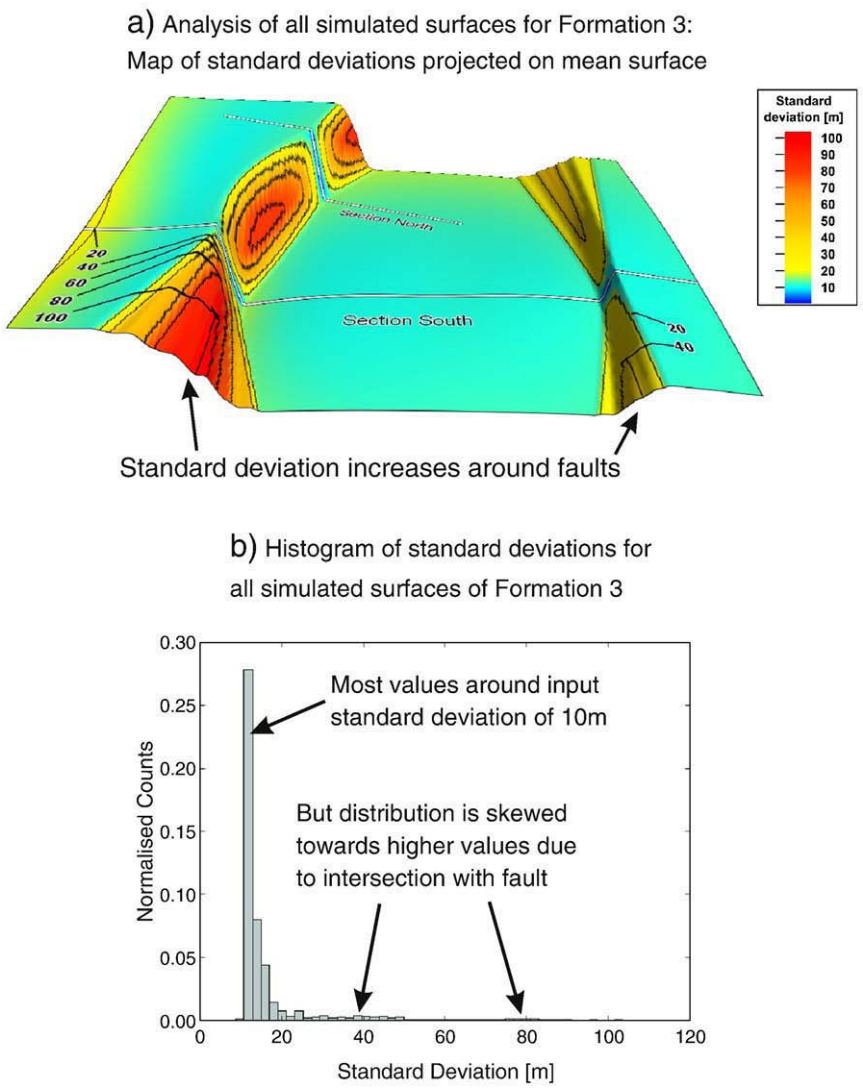

Fig. 7. Map-based statistical analysis for elevation surface structures: (a) contour plot of standard deviations of all simulated surfaces for top of Formation 3, projected onto the mean of these surfaces; the standard deviation increases significantly around the faults above the input value of 10 m; this is also visible in (b) a histogram of standard deviations at all map positions: the distribution is skewed towards higher values.

structure is overturned and may be a multivalued function at each location, i.e. the formation boundary is present more than once along a vertical line (see Fig. 1d for a schematic view and Fig. 8 for a representation of the example model). We now have the case of a full three-dimensional geological setting. This model extends 1000 m in the East–West, the North–South, and also in the depth direction. Fig. 8 shows a 3D visualisation of this model and the two orthogonal cross-sections where input data points and orientations are defined.

3.2.2. Simulation parameters and settings

In this example, we want to evaluate the application of our method to the complex doming structure. We are thus only changing the parameters affecting the dome unit. Also, we assign the same probability distributions to all points and orientation measurements (see Table 2). Again, we perform 20 simulation runs.

3.2.3. Analysis and visualisation of results

Processing the results is not as simple as in the first model since we are now dealing with a full 3D setting. We can still plot all modelled realisation surfaces as lines within a section but the representation and analysis in a depth-to-surface plot (as in Fig. 7a) or similar map views are no longer feasible.

We thus use here the indicator function methods introduced above (Section 2.5). In this case, we export all simulated models into a regular (voxel) grid with cell dimensions of $20 \times 20 \times 20$ m. We then apply Eq. (8) to all simulations of the dome unit and obtain 20 discrete indicator functions. Taking the sum of all functions at each cell (Eq. (11)), we derive an indicator probability estimate for the dome unit (based on these 20 simulations) as a scalar function in 3D, describing the probability that the dome exists at this grid cell.

We can visualise these estimates in cross-sections or as isosurfaces of probability in 3D. Fig. 9a shows the surface contour of the minimal extent and maximal extent of all simulated domes. In the cross-section, isolines of different probability values are plotted. As both visualisations are based on the same scalar function, they are completely self-consistent.

The analysis above provides an estimate of the probability to have a unit at any one point in space. Still, in many cases, it is important to know where the boundary of a unit is. Therefore, we apply Eq. (12) to derive the absolute value of the gradient of this field. This provides a measure of the probability to encounter a boundary (Fig. 9b) with high values indicating high probability.

Please cite this article as: Wellmann, J.F., et al., Towards incorporating uncertainty of structural data in 3D geological inversion, Tectonophysics (2010), doi:10.1016/j.tecto.2010.04.022

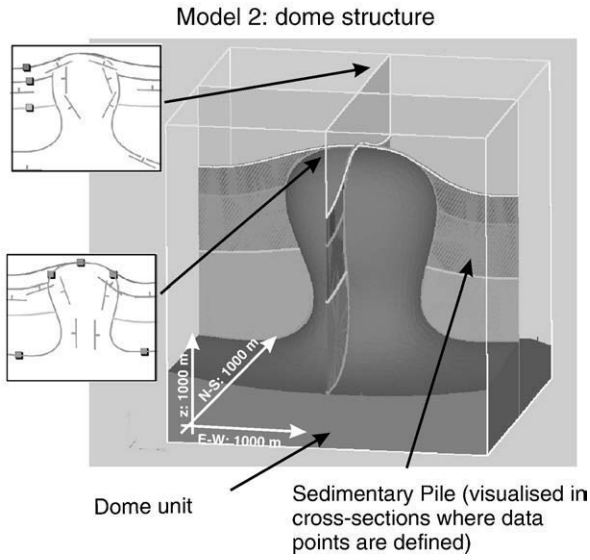

Fig. 8. Evaluation Model 2: complex full three-dimensional dome structure; data are defined in two orthogonal cross-sections (insets).

A further possibility would be to analyse a specific model feature, for example the different volumes for all simulated dome models, using Eq. (13).

4. Discussion

We have shown that it is possible to quantitatively evaluate uncertainties in 3D geological modelling that are introduced by imprecision in different types of input data. The main feature of our analysis is that we perform all simulations based on statistical manipulations (i.e. sampling from the distributions) of the input data. These can be orientation measurements and formation or fault contact points. Such data usually are the basis for all types of structural geological modelling, from observations in the field, to those in a drillhole or those indirectly interpreted in a seismic profile. Assigning uncertainties to these data types is thus close to geological thinking. The same applies to the complete workflow which is simple and straight-forward, starting from an initial model, creating several model representations and finally comparing them. We think that this is an important step to enable a 3D uncertainty estimation and interpretation of geological models for the non-expert in an intuitive way.

The approach is simple, intuitive and still applicable in both structurally simple and complex geological models. As our simulation is based on the full 3D potential-field interpolation method (Lajaunie et al., 1997; Calcagno et al., 2008), we are not limited to structural settings where only one value can be defined at every location as in the case of elevation surface/2.5D representations (see Fig. 1a and the approaches of Thore et al., 2002; Turner, 2006; Bistacchi et al., 2008; Suzuki et al., 2008). In the two presented examples, we have shown how we can apply the method to a simple graben-type setting and to a complicated dome structure. These models are kept simple to show the application of the method. Still, the uncertainty simulation can be applied to all cases where the implicit potential-field approach can be used for modelling. Complex modelling examples have been presented in the literature (e.g. Maxelon and Mancktelow, 2005; Putz et al., 2006; Calcagno et al., 2008; Joly et al., 2008). The advantage of our method is that it is not limited to a specific geological setting and that the workflow itself is always performed in the same way.

Table 2
Estimations of the standard deviation assigned to the data in the dome model.

Formation	Data type	Direction	Stdev
Dome unit	Surface contact point	Depth (z)	20 m
Dome unit	Orientation	Dip angle	5°

The main difference in the application of our approach for simple and complex settings is the visualisation and analysis of the results. Simple visualisation techniques, like representation of all simulated surfaces in one section or map view and occurrence histogram of a surface intersection in a drillhole can directly be applied in many cases (see example in Fig. 6). A statistical analysis of the simulation results can be applied, for example to estimate the maximum and minimum extent or mean and standard deviation of a surface at depth (Fig. 7).

In complex settings, the results of the uncertainty simulation can be visualised with the use of indicator functions in full 3D. The dome model (Section 3.2) is an example where this method is used to visualise the maximum change of models in the simulation run, highlighting the areas of highest uncertainties. These visualisation techniques can be extended to include all formations of a model and to derive further measures, like the minimum and maximum extent (Fig. 9a) or the probability to encounter the boundary (Fig. 9b) of a modelled formation. They can also directly be used to represent the uncertainties in the volume estimation for one formation (Eq. (13)). This is of great interest in many exploration situations. The use of indicator functions is a powerful method to analyse and visualise uncertainties in complex settings.

Limitations of our method are mainly related to the geological modelling technique itself. The modelling can become slow when very large data sets are used. In these cases, it could be reasonable to subdivide the model range into smaller areas for the uncertainty simulation. Still, since our approach is ideal for parallel implementation, the whole uncertainty estimation will, when optimized and performed on a suitable computer, only take minimally longer than one model run.

As our method is primarily targeting uncertainties in the input data (i.e. uncertainties of Type I, Fig. 2a), the analysis is mainly representative of areas where data are available. In-between and away from data points an additional uncertainty exists, the problem of correct interpolation and extrapolation (Type II, Fig. 2b). This uncertainty is strongly related to the modelling interpolation technique. For the implicit potential-field interpolation that we apply, this uncertainty has been evaluated by Aug (2004) and Chilès et al. (2004). Uncertainties due to incomplete geological knowledge (Type III, Fig. 2c) are very hard to assess but could partly be integrated into our simulation, e.g. the existence of a fault could be included on a probabilistic basis (see Appendices A). Thus, even if our method is currently mainly focused on Type 1 uncertainty – the imprecision of the raw data – it can be combined and extended to other types for a comprehensive evaluation of model uncertainty.

Apart from the applications of our method described above, the presented examples also suggest that it is important to analyse uncertainties introduced by the input data and their influence on each other. The analysis of results for Model 1 in Fig. 7a shows how the uncertainty of the dip direction of the faults and the formation tops interact. The resulting uncertainty for the formation tops exceeds the assumed input standard deviation significantly in this simple example (Fig. 7b). We thus conclude that it is not sufficient to assign a simple statistical measure to a simulated surface, derived from input data distributions, but that it is important to consider all input data uncertainties and their interaction. Our method provides a possibility to achieve this.

In addition to the visualisation of uncertainties, the simulated models can also be used directly as an input for further simulation and inversion techniques. It is common practice to use a 3D structural model as an input for geophysical simulations, like stress-field analyses or fluid and heat flow studies. And even though it is accepted that the geological basis model itself is a major source of

Please cite this article as: Wellmann, J.F., et al., Towards incorporating uncertainty of structural data in 3D geological inversion, Tectonophysics (2010), doi:10.1016/j.tecto.2010.04.022

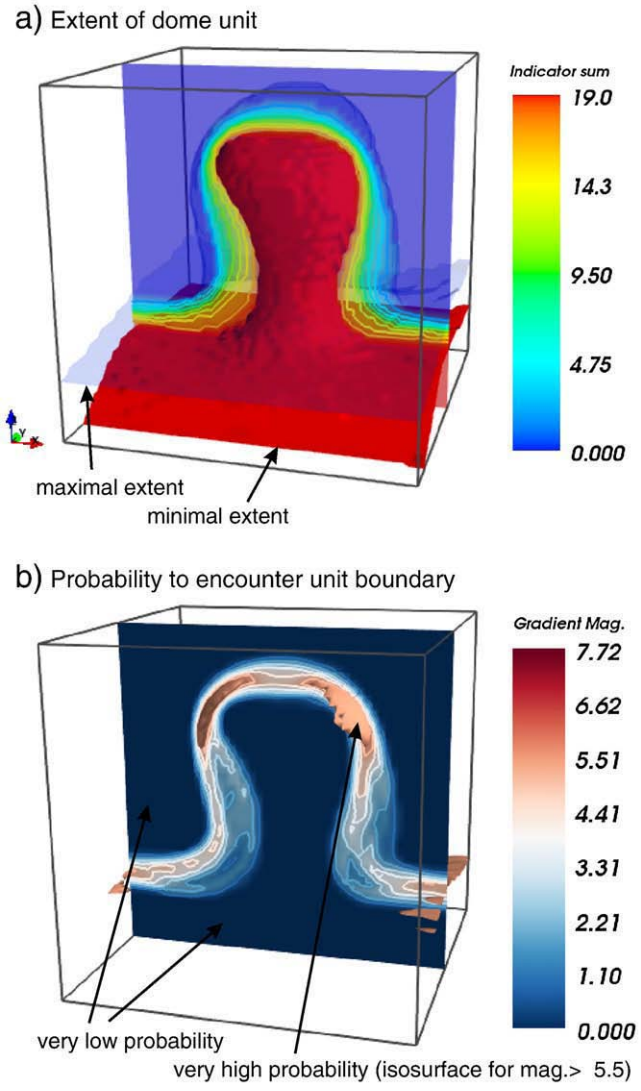

Fig. 9. Visualisation of results for Evaluation Model 2, complex structures: (a) representation of minimal and maximal extent of the dome unit for all simulated models; the analysis is performed using indicator functions, the indicator sum is a measure of the probability to encounter the unit in a cell (b) gradient magnitude of the indicator field in (a), calculated with Eq. (**12**); this provides a measure of the probability to encounter the unit boundary in full 3D.

uncertainty in these simulations (e.g. Subbey et al., 2004; Caumon et al., 2009), it is usually not evaluated. With our method we can directly use a variety of different model realisations as input. We are thus respecting the possible uncertainties in the geological model for further simulations. The geophysical simulations can then be performed in the light of the quality of the geological model. For example, we plan to use the created range of models as a direct input for geothermal simulations.

This type of combination of structural modelling with other types of complex data (e.g. fluid flow simulations) has been identified by Caumon et al. (2009) as an important direction of current research. For example, Suzuki et al. (2008) proposed a method to use reservoir production data to identify possible structural interpretations. Our approach is similar to this method on a conceptual level. But whereas Suzuki et al. (2008) and other approaches (typically implemented in oil exploration and production software) concentrate on structural modelling derived from seismic data, our approach is suitable to all types of input data, including orientation measurements. Also, our method is not limited to typical sedimentary settings as encountered in oil exploration but suitable for complex 3D settings in any geological environment. And as we perform all simulations directly based on parameterised structural measurements, the effect of every single measurement can be analysed. Our structural uncertainty measure is also quite distinct from other lithological uncertainty measures where the focus is classically laid on inversion of properties assigned to grid cells (e.g. Guillen et al., 2008) with respect to assigned properties based on geophysical observations (e.g. magnetics and gravity) but does not incorporate the parameterised uncertainty of the structural measurements themselves. We call this classical method geophysically based inversion whereas ours would be more correctly labelled as geologically based inversion. Both techniques complement each other and can be used in tandem. In this sense, our method opens-up the way to a unified geological and geophysical data-driven ensemble modelling and inversion.

Our uncertainty simulation scripts will be distributed free of charge for all scientific purposes. Please contact the corresponding author for a copy of the program and further information. An evaluation license for the software GeoModeller is available on the website http://www.geomodeller.com.

Acknowledgements

We are thankful for the constructive, helpful and motivating comments of three anonymous reviewers. This work was enabled by an Australian International Postgraduate Research Scholarship (IPRS) and a Top-up Scholarship from Green Rock Energy Ltd. We thank Antonio Guillen and Gabriel Courrioux for helpful discussions and kind support. Soazig Corbel and Aurore Joly were a great help with their knowledge about 3D modelling. The Western Australian Geothermal Centre of Excellence (WAGCoE) is a joint centre of Curtin University, The University of Western Australia and the CSIRO and funded by the State Government of Western Australia.

Appendix A. Inverse Problems, Conditional Simulations, and Uncertainties for Models of the Class Considered in this Paper

The method described in this paper is closely related to the formulation of the "forward part" of an inverse problem for the interpolation. It is also similar to the technique of conditional simulation of geostatistics (e.g. Chilès and Delfiner, 1999). We make these analogies more precise here.

We assume a set of pre-defined functions that we apply to perform the interpolation, specifically the harmonic potential-field method (Lajaunie et al., 1997). Other functions are related to the functional form of the variogram for conditional simulation in geostatistics, the Radial Basis Functions for interpolation or the Green's functions used to specify a Boundary Value Problem. If we denote those pre-defined functions of position by $f_i(\boldsymbol{x})$, then the subscript i indexes the admissible set of functions, and $\boldsymbol{x}$ is the position vector at which the interpolation is evaluated. There are some additional parameters to consider:

$$f_i\left(\boldsymbol{x}; k_j, \alpha_k, \beta_\ell\right).$$

Here, the k_j parameterise the set of positions and attitudes of control points (e.g. the depth and orientation of a contact between geological units in a borehole, see also Section 2.2). The quantities α_k are members of the set of additional parameters of the interpolation function (e.g. a parameterisation of the range, sill, and nugget effect in a geostatistical variogram). Finally, the β_ℓ parameterise a partitioning of space inside of which the individual f_i are valid, like the compartments between faults.

The difference between the present work and that of Chilès and Delfiner (1999) and Aug (2004) is that we vary the k_j (Eqs. (1), (6)), and they vary the α_k. Neither study has attempted to vary the

$\beta_{\swarrow}$, but any combination of these variations for the forward problem is valid. Additionally, either an inverse problem or a geostatistical conditional simulation could be formulated to vary any or all of the f_i, k_j, α_k, and $\beta_{\swarrow}$, or indeed any other appropriate parameter.

For concreteness, with reference to Section 1.2 and Fig. 2, we identify uncertainties in the k_j as uncertainties of Type 1, uncertainties in the α_k as those of Type 2, and uncertainties in $\beta_{\swarrow}$ as those of Type 3 following the classification of Mann (1993).

Appendix B. Supplementary data

Supplementary data associated with this article can be found, in the online version, at doi:10.1016/j.tecto.2010.04.022.

References

Aug, C., 2004. Modélisation géologique 3D et caractérisation des incertitudes par la méthode du champ de potentiel: PhD thesis. ENSMP, Paris.

Bárdossy, G., Fodor, J., 2001. Traditional and new ways to handle uncertainty in geology. Natural Resources Research 10 (3), 179–187.

Bistacchi, A., Massironi, M., Dal Piaz, V.G., Monopoli, B., Schiavo, A., Toffolon, G., 2008. 3D fold and fault reconstruction with an uncertainty model: an example from an Alpine tunnel case study. Computers & Geosciences 34 (4), 351–372.

Calcagno, P., Chilès, J.-P., Courrioux, G., Guillen, A., 2008. Geological modelling from field data and geological knowledge: part I. modelling method coupling 3D potential-field interpolation and geological rules: recent advances in computational geodynamics: theory, numerics and applications. Physics of the Earth and Planetary Interiors 171 (1–4), 147–157.

Caumon, G., Collon-Drouaillet, P., Carlier, Le., de Veslud, C., Viseur, S., Sausse, J., 2009. Surface-based 3D modeling of geological structures. Mathematical Geosciences 41 (8), 927–945.

Chilès, J.-P., Delfiner, P., 1999. Geostatistics: Modeling Spatial Uncertainty. A Wiley-Interscience Publication. Wiley, New York, NY.

Chilès, J.-P., Aug, C., Guillen, A., Lees, T., 2004. Modelling of geometry of geological units and its uncertainty in 3D from structural data: the potential-field method. Orebody Modelling and Strategic Mine Planning — Uncertainty and Risk Management Models. Spectrum Series, 14. Australasian Institute of Mining and Metallurgy, Carlton, Victoria, pp. 329–336.

Courrioux, G., Nullans, S., Guillen, A., Boissonnat, D.J., Repusseau, P., Renaud, X., Thibaut, M., 2001. 3D volumetric modelling of Cadomian terranes (Northern Brittany, France): an automatic method using Voronoi diagrams. Tectonophysics 331 (1–2), 181–196.

Cox, A.L., 1982. Artifactual uncertainty in risk analysis. Risk Analysis 2 (3), 121–135.

Davis, C.J., 2002. Statistics and Data Analysis in Geology, 3rd Edition. Wiley, New York, NY.

Deutsch, V.C., 2002. Geostatistical Reservoir Modeling. Oxford University Press, New York.

Fisher, R., 1953. Dispersion on a sphere. Proceedings of the Royal Society of London. Series A, Mathematical and Physical Sciences 217 (1130), 295–305.

Frank, T., Tertois, A.-L., Mallet, J.-L., 2007. 3D-reconstruction of complex geological interfaces from irregularly distributed and noisy point data. Computers & Geosciences 33 (7), 932–943.

Galera, C., Bennis, C., Moretti, I., Mallet, J.-L., 2003. Construction of coherent 3D geological blocks. Computers & Geosciences 29 (8), 971–984.

Glinsky, E.M., Asher, B., Hill, R., Flynn, M., Stanley, M., Gunning, J., Thompson, T., Kalifa, J., Mallat, S., White, C., 2005. Integration of uncertain subsurface information into multiple reservoir simulation models. The Leading Edge 24 (10), 990–999.

Goodchild, F.M., Buttenfield, B., Wood, J., 1994. Introduction to visualizing data validity. In: Hearnshaw, M.H., Unwin, J.D. (Eds.), Visualization in Geographical Information Systems. John Wiley & Sons, pp. 141–149.

Goovaerts, P., 1997. Geostatistics for Natural Resources Evaluation. Oxford University Press.

Guillen, A., Calcagno, P., Courrioux, G., Joly, A., Ledru, P., 2008. Geological modelling from field data and geological knowledge: part II. modelling validation using gravity and magnetic data inversion: recent advances in computational geodynamics: theory, numerics and applications. Physics of the Earth and Planetary Interiors 171 (1–4), 158–169.

Howard, S.A., Hatton, B., Reitsma, F., Lawrie, I.G.K., 2009. Developing a geoscience knowledge framework for a national geological survey organisation: geoscience knowledge representation in cyberinfrastructure. Computers & Geosciences 35 (4), 820–835.

Joly, A., Martelet, G., Chen, Y., Faure, M., 2008. A multidisciplinary study of a syntectonic pluton close to a major lithospheric-scale fault—relationships between the Montmarault granitic massif and the Sillon Houiller Fault in the Variscan French Massif Central: 2. gravity, aeromagnetic investigations, and 3-D geologic modeling. Journal of Geophysical Research 113, B01404.

Kessler, H., Mathers, S., Sobisch, H.-G., 2009. The capture and dissemination of integrated 3D geospatial knowledge at the British Geological Survey using GSI3D software and methodology. Computers & Geosciences 35 (6), 1311–1321.

Lajaunie, C., Courrioux, G., Manuel, L., 1997. Foliation fields and 3D cartography in geology: principles of a method based on potential interpolation. Mathematical Geology 29 (4), 571–584.

MacEachren, M.A., Robinson, A., Hopper, S., Gardner, S., Murray, R., Gahegan, M., Hetzler, E., 2005. Visualizing geospatial information uncertainty: what we know and what we need to know. Cartography and Geographic Information Science 32 (3), 139–161.

Malengreau, B., Lénat, J.-F., Froger, J.-L., 1999. Structure of Réunion Island (Indian Ocean) inferred from the interpretation of gravity anomalies. Journal of Volcanology and Geothermal Research 88 (3), 131–146.

Mallet, J.-L., 1992. Discrete smooth interpolation in geometric modelling. Computer-Aided Design 24 (4), 178–191.

Mann, J.C., 1993. Uncertainty in geology. Computers in Geology—25 Years of Progress. Oxford University Press, pp. 241–254.

Martelet, G., Calcagno, P., Gumiaux, C., Truffert, C., Bitri, A., Gapais, D., Brun, P.J., 2004. Integrated 3D geophysical and geological modelling of the Hercynian Suture Zone in the Champtoceaux area (south Brittany, France). Tectonophysics 382 (1–2), 117–128.

Maxelon, M., Mancktelow, S.N., 2005. Three-dimensional geometry and tectonostratigraphy of the Pennine zone, Central Alps, Switzerland and Northern Italy. Earth-Science Reviews 71 (3–4), 171–227.

Moretti, I., 2008. Working in complex areas: new restoration workflow based on quality control, 2D and 3D restorations. Marine and Petroleum Geology 25 (3), 205–218.

Putz, M., Stuwe, K., Jessell, M., Calcagno, P., 2006. Three-dimensional model and late stage warping of the Plattengneis Shear Zone in the Eastern Alps. Tectonophysics 412 (1–2), 87–103.

Sander, K.B., Cawthorn, G.R., 1996. 2.5-D gravity model of the Ni–Cu–PGM mineralized Mount Ayliff Intrusion (Insizwa Complex), South Africa. Journal of Applied Geophysics 35 (1), 27–43.

Subbey, S., Christie, M., Sambridge, M., 2004. Prediction under uncertainty in reservoir modeling: risk analysis applied to petroleum exploration and production. Journal of Petroleum Science and Engineering 44 (1–2), 143–153.

Suzuki, S., Caumon, G., Caers, J., 2008. Dynamic data integration for structural modeling: model screening approach using a distance-based model parameterization. Computational Geosciences 12 (1), 105–119.

Tacher, L., Pomian-Srzednicki, I., Parriaux, A., 2006. Geological uncertainties associated with 3-D subsurface models. Computers & Geosciences 32 (2), 212–221.

Thore, P., Shtuka, A., Lecour, M., Ait-Ettajer, T., Cognot, R., 2002. Structural uncertainties: determination, management, and applications. Geophysics 67 (3), 840–852.

Truffert, C., Egal, E., Le Goff, E., Courrioux, G., Guennoc, P., 2001. Gravity modellings of the Cadomian active margin of northern Brittany. Tectonophysics 331 (1–2), 81–97.

Turner, A., 2006. Challenges and trends for geological modelling and visualisation. Bulletin of Engineering Geology and the Environment 65 (2), 109–127.

Viard, T., Caumon, G., Levy, B., 2007. Uncertainty visualization in geological grids. 27th Gocad Meeting 2007, pp. 1–21.

Wu, Q., Xu, H., Zou, X., 2005. An effective method for 3D geological modeling with multi-source data integration. Computers & Geosciences 31 (1), 35–43.

Wycisk, P., Hubert, T., Gossel, W., Neumann, C., 2009. High-resolution 3D spatial modelling of complex geological structures for an environmental risk assessment of abundant mining and industrial megasites: 3D modeling in geology. Computers & Geosciences 35 (1), 165–182.

Please cite this article as: Wellmann, J.F., et al., Towards incorporating uncertainty of structural data in 3D geological inversion, Tectonophysics (2010), doi:10.1016/j.tecto.2010.04.022